Orbital control on carbon cycle and oceanography in the mid-Cretaceous greenhouse

Martino Giorgioni,[1] Helmut Weissert,[1] Stefano M. Bernasconi,[1] Peter A. Hochuli,[1,2] Rodolfo Coccioni,[3] and Christina E. Keller[1]

Received 9 May 2011; revised 2 November 2011; accepted 20 November 2011; published 21 January 2012.

[1] We established a new high-resolution carbonate carbon isotope record of the Albian interval of the Marne a Fucoidi Formation (Central Apennines, Italy), which was deposited on the southern margin of the western Tethys Ocean. Bulk carbonate sampled with 10–15 cm spacing was used for the construction of a continuous carbon isotope curve through the Albian stage. Spectral analyses reveal prominent 400 kyr cyclicity in the $\delta^{13}C$ curve, which correlates with Milankovitch long eccentricity changes. Cycles occurring in our record resemble those observed in several Cenozoic $\delta^{13}C$ records, suggesting that a link between orbital forcing and carbon cycling existed also under mid-Cretaceous greenhouse conditions. Based on comparisons with Cenozoic eccentricity-carbon cycle links we hypothesize that 400 kyr cycles in the mid-Cretaceous were related to a fluctuating monsoonal regime, coupled with an unstable oceanic structure, which made the oceanic carbon reservoir sensitive to orbital variations. In the Tethys these oceanographic conditions lasted until the Late Albian, and then were replaced by a more stable circulation mode, less sensitive to orbital forcing.

Citation: Giorgioni, M., H. Weissert, S. M. Bernasconi, P. A. Hochuli, R. Coccioni, and C. E. Keller (2012), Orbital control on carbon cycle and oceanography in the mid-Cretaceous greenhouse, *Paleoceanography*, *27*, PA1204, doi:10.1029/2011PA002163.

1. Introduction

[2] The Cretaceous is known for its extreme greenhouse climatic conditions: temperatures were very warm, especially at the poles, atmospheric pCO_2 was several times higher than today, and sea level was the highest of the last 200 million years. These conditions peaked in the mid-Cretaceous: between the Aptian and the Turonian [e.g., *Huber et al.*, 2002; *Pucéat et al.*, 2003; *Bice and Norris*, 2002; *Bice et al.*, 2006; *Hardenbol et al.*, 1998].

[3] In the Tethys and in the Atlantic Ocean deep-water sediments formed during the mid-Cretaceous are often rich in black-shales, but also include oceanic red beds and almost purely white micritic limestones, especially from the Late Albian onward [e.g., *Cool*, 1982; *Arthur and Premoli Silva*, 1982; *Hu et al.*, 2006; *Hay*, 2008]. These sediments often occur in alternating lithological couplets and bundles related to orbitally driven climatic variations [e.g., *Dean et al.*, 1977; *Gale*, 1989; *Fischer et al.*, 1991; *Prokoph and Thurow*, 2001]. These red, black, and white pelagic sediments, which were widespread in the Cretaceous, have only few analogs in the Cenozoic and today, testifying to very different oceanographic and climatic conditions and strong orbital forcing on climate at that time.

[4] High-resolution investigations of Cenozoic deep-water archives have shown a strong match between stable carbon isotope records and 400 kyr cycling, corresponding to the long eccentricity of Milankovitch orbital cycles [e.g., *Zachos et al.*, 2001; *Cramer et al.*, 2003; *Holbourn et al.*, 2005; *Pälike et al.*, 2006; *Wang et al.*, 2010]. Although the 400 kyr period is strong and consistent in carbon isotope records, it is still not clear how orbital changes are linked to the carbon cycle. New insights into these mechanisms may come from testing whether they were limited to Cenozoic climatic conditions or if carbon cycle – eccentricity links existed also in the hothouse Cretaceous climate.

[5] During the Cretaceous, the carbon cycle was affected by major perturbations related to intense volcanism and possibly sudden methane bursts [e.g., *Larson and Erba*, 1999; *Jahren et al.*, 2001; *Weissert and Erba*, 2004; *Méhay et al.*, 2009], however, some studies suggest that orbital forcing played also a role in carbon cycling [*Sprovieri et al.*, 2006; *Voigt et al.*, 2007].

[6] In this study we follow and discuss the paleoclimatic implications of the hypothesis proposed by *Voigt et al.* [2007] that in the Cretaceous the global carbon cycle was affected by orbital forcing as it is documented for the Cenozoic. We will add to an improved understanding of carbon cycling and major forcing mechanisms at a time of

[1]Department of Earth Sciences, Geological Institute, ETH Zurich, Zurich, Switzerland.
[2]Palaeontological Institute, University of Zurich, Zurich, Switzerland.
[3]Dipartimento di Scienze della Terra, della Vita e dell'Ambiente, Università di Urbino, Urbino, Italy.

0883-8305/12/2011PA002163

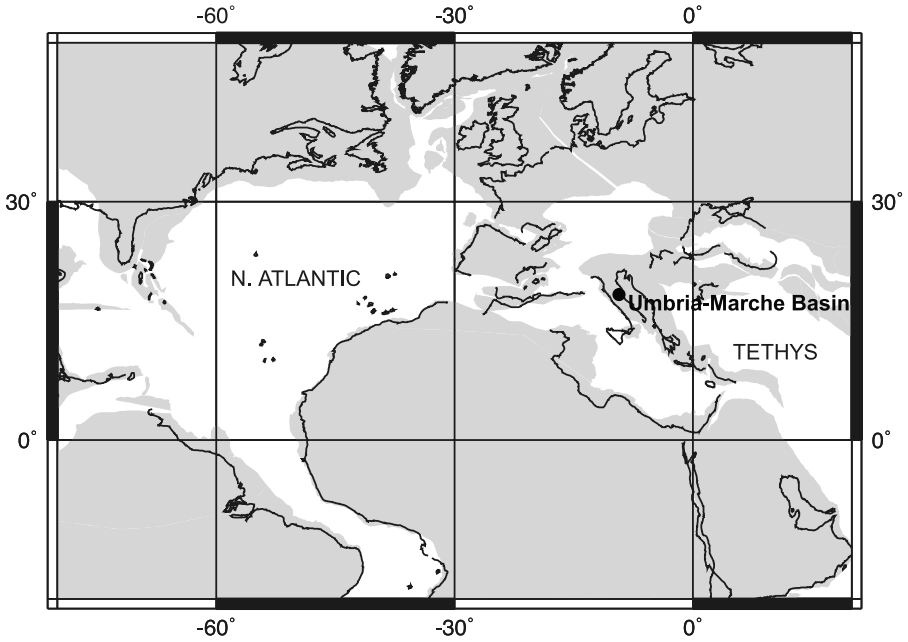

Figure 1. Paleogeographic map of the North Atlantic and the western Tethys during the Late Albian, with the location of the studied area (created with Geomar map generator www.odsn.de).

repeated volcanically induced perturbations of the global carbon cycle.

2. Geological Setting

[7] The studied section is located in the Umbro-Marchean Apennines, in Central Italy, where an uninterrupted sedimentary history from the late Triassic to the late Miocene is preserved [*Lavecchia and Pialli*, 1989]. This succession formed in a deep basin located on the Adria margin, in the southern part of the western Tethys (Figure 1). The section presented here is composed of two segments, which were measured at two sites located about 20 km apart (Figure 2).

[8] In this study we focus on the Marne a Fucoidi Formation, which represents the Aptian-Albian interval of the Umbria Marche succession (Figure 3). We investigate the Albian interval of this formation, which is about 40 m thick and consists of variegated pelagic limestones and marlstones, rhythmically alternating with black shales. These alternating facies are arranged in lithological couplets, bundles, and superbundles, which match with Milankovitch precession, short-eccentricity, and long eccentricity, respectively [*Herbert and Fischer*, 1986; *Tornaghi et al.*, 1989; *Fischer et al.*, 1991; *Fiet et al.*, 2001; *Grippo et al.*, 2004]. The succession includes also some 1 to 3 m thick red beds. The Marne a Fucoidi Formation is overlain by the Scaglia Bianca Formation, which instead consists of homogenous whitish, sometimes reddish, pelagic limestones, with chert (Figures 3 and 4).

3. Sections Studied

3.1. Piobbico Core

[9] The Piobbico core was drilled in the town of Piobbico, along the Apecchiese road, in 1982 (Figure 2). It encompasses the whole Marne a Fucoidi Formation and is one of the most detailed records of the Aptian-Albian [e.g., *Herbert and Fischer*, 1986; *Tornaghi et al.*, 1989; *Erba*, 1992; *Grippo et al.*, 2004]. The Albian interval of the Piobbico core is about 40m thick and ends in the *Rotalipora ticinensis* zone, whereas the *Rotalipora appenninica* zone (uppermost Albian) is missing [*Tornaghi et al.*, 1989; *Grippo et al.*, 2004]. The base of the Albian in the core is not clearly defined because of some uncertainty in biostratigraphy [*Tornaghi et al.*, 1989; *Grippo et al.*, 2004] and because of a still poorly defined base of the Albian in the chronostratigraphic time scale [*Gale et al.*, 2011]. Based on calcareous nannofossils and carbon isotope stratigraphic data, *Tiraboschi et al.* [2009] placed the base of the Albian close

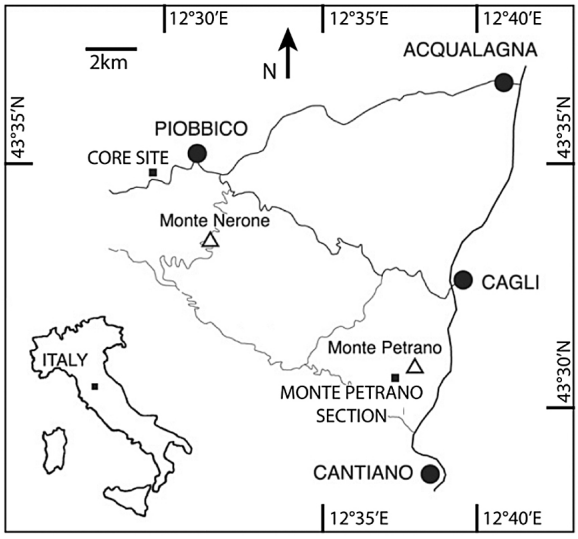

Figure 2. Geographic locations of the studied sections [after *Grippo et al.*, 2004].

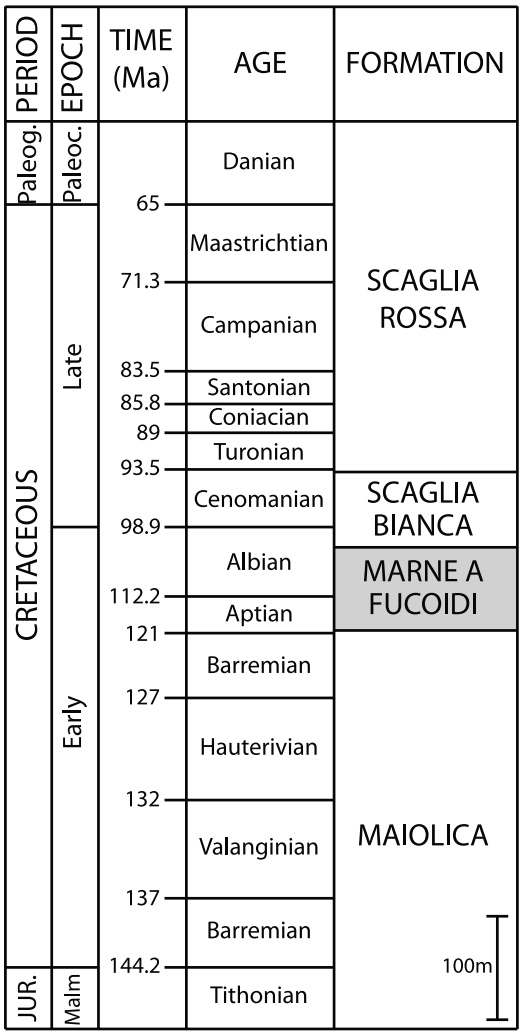

Figure 3. Lithostratigraphic units of the Cretaceous sedimentary sequence of the Umbria-Marche basin, based on data by *Coccioni* [1996]. The Marne a Fucoidi Formation is highlighted in gray.

to the base of the *Ticinella primula*/*Hedbergella rischi* zone, at 40.14 m of the Piobbico core. As we include the data from *Tiraboschi et al.* [2009] in this study we follow their choice for the position of the base of the Albian.

3.2. Monte Petrano

[10] The Monte Petrano section is located on the southwestern side of Monte Petrano, next to the town of Cagli (Figure 2). It encompasses a large part of the Cretaceous succession, from the Marne a Fucoidi to the Scaglia Rossa Formations (Figure 3). *Fiet et al.* [2001] obtained a biostratigraphic zonation of the Albian interval of the Marne a Fucoidi Formation correlating this section with others studied by previous authors in surrounding localities [*Premoli Silva and Sliter*, 1995; *Coccioni et al.*, 1989].

[11] In this study we considered only the upper 29 m of the Marne a Fucoidi Formation from this section because the lower part of the Albian interval, consisting mainly of a marly lithology, is less well-preserved and cannot be sampled in the same detail as the upper part. According to the biostratigraphic zonation of *Premoli Silva and Sliter* [1995] and *Coccioni et al.* [1989], adapted by *Fiet et al.* [2001], our studied interval begins in the lower *Biticinella breggiensis* zone and ends at the top of the *Rotalipora ticinensis* zone, including the lowermost Scaglia Bianca Formation (Figure 4).

3.3. Correlation Between the Studied Sections

[12] As the lower part of the Albian interval of the Marne a Fucoidi Formation in Monte Petrano was not suitable for our high-resolution study we completed the record by using the data of *Tiraboschi et al.* [2009] from the Piobbico core. *Tiraboschi et al.* [2009] excluded the uppermost 8 m of the core from their data set because of poor core recovery. In addition, although the original recovery of the Piobbico core was very good, the intense sampling during the last thirty years consumed some parts completely. Therefore, in order to obtain the most complete record possible we combined the best-preserved parts of the two sections. We chose the base of the second red limestone bed, which is clearly present in both sections, for core-outcrop correlation. In the resulting composite section the Albian Marne a Fucoidi interval is 40 m thick: 17 m in the Piobbico core (lower part) and 23 m in the outcrop section at Monte Petrano (Figure 4). The Monte Petrano segment is totally continuous, whereas a fault occurs 13 m above the base of the Piobbico core segment. *Tiraboschi et al.* [2009] accounted for a gap of 50 cm due to this fault.

[13] According to biostratigraphic and cyclostratigraphic models this interval encompasses a time span of about 8 Myr [*Premoli Silva and Sliter*, 1995; *Grippo et al.*, 2004]. The upper part of the data set of *Tiraboschi et al.* [2009] is 15 m thick and corresponds to about two thirds of the Monte Petrano segment. Correlations of the Marne a Fucoidi Formation across the Umbria-Marche basin showed that the succession in Monte Petrano is some meters thicker than in the Piobbico core. This difference is due to condensed or missing layers at a centimetric scale in the Piobbico core [*Fiet*, 1998; *Grippo et al.*, 2004]. However, these discrepancies are within the uncertainty of sampling in this study, so they do not significantly affect the continuity of the record.

4. Methods

4.1. Carbon and Oxygen Isotope Geochemistry

[14] The Monte Petrano section was sampled for carbon isotope analyses with an average resolution of a sample every 10 cm. Carbon and oxygen isotopic composition of the bulk carbonate was measured in the isotope-geochemistry laboratory of the ETH-Zurich using a GasBench II system coupled to a Delta V mass spectrometer (Thermo Fisher Scientific, Bremen, Germany). About 350 μg of powdered sample were placed in 12 ml vacutainers, flushed with helium and then reacted with 5 drops of 100% phosphoric acid at 72°C. The instrument is calibrated with the international reference materials NBS 19 ($\delta^{13}C = +1.95‰$, $\delta^{18}O = -2.2‰$) and NBS 18 ($\delta^{13}C = -5.05‰$, $\delta^{18}O = -23.1‰$). Values are reported in the conventional delta notation with respect to VPDB. Analytical reproducibility as 1 std deviation of the mean of the standards used in the runs is $\pm 0.05‰$ for carbon and $\pm 0.08‰$ for oxygen values. Carbon isotope values of the Piobbico core segment are from *Tiraboschi*

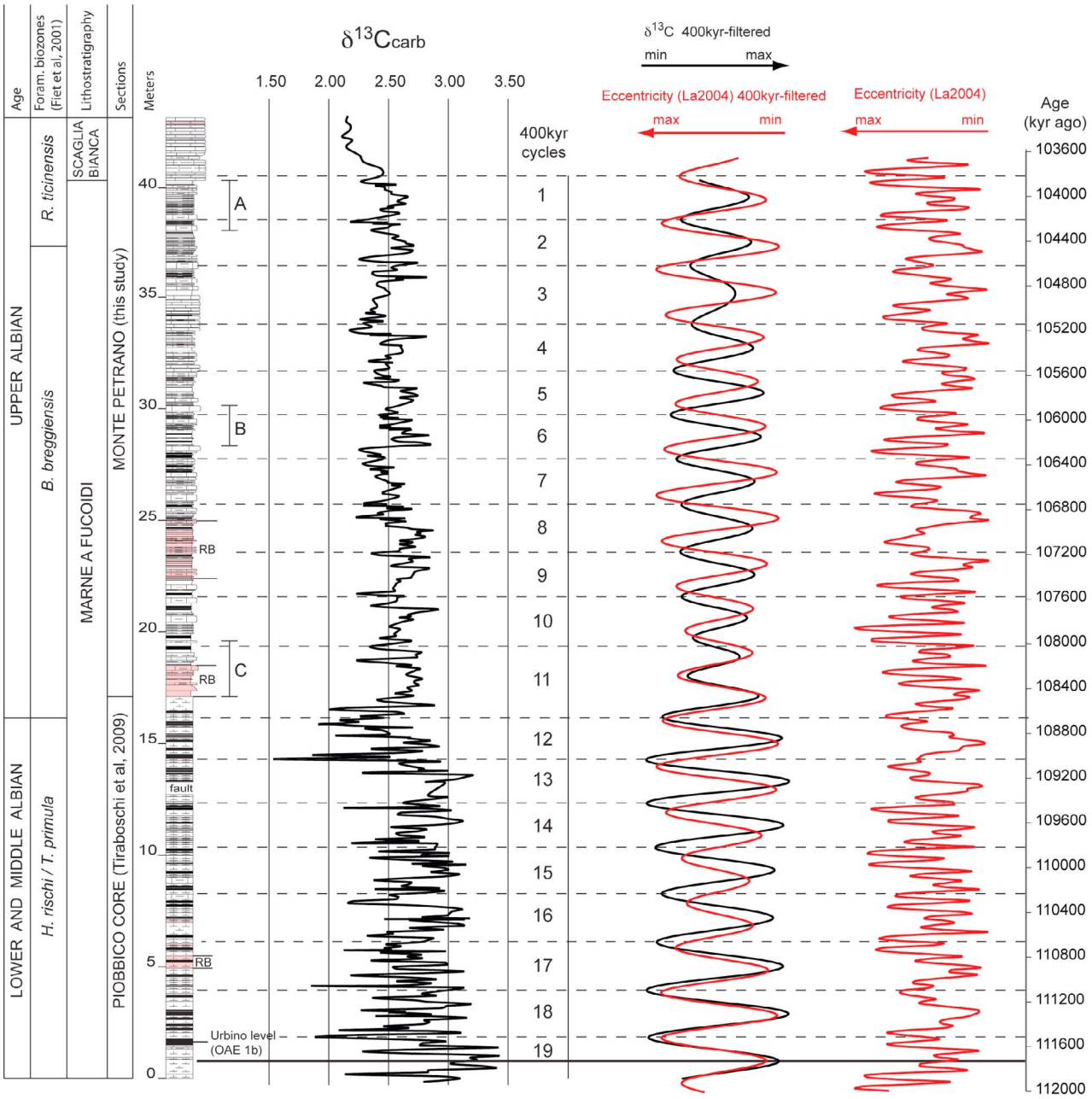

Figure 4. Lithological log, $\delta^{13}C$ curve, numbers of 400 kyr cycles, 400 kyr-filtered $\delta^{13}C$ (black line) and eccentricity (red line) curves, and La2004 eccentricity curve. Note that the eccentricity curves are reversed on the *x* axis in order to better visualize the coupling between $\delta^{13}C$ maxima and eccentricity minima. The black line at cycle 19 shows where the two filtered curves are tied. RB indicates red beds. Intervals A, B, and C are those in which also $CaCO_3$ content has been measured.

et al. [2009]. They are at the same stratigraphic resolution of about a sample per 10 cm.

4.2. Spectral Analyses

[15] We performed spectral analyses on carbon isotope data using MATLAB R2010a, adapting the procedures described by *Trauth* [2010]. We performed the calculations both on the whole series and on each segment of the section separately.

[16] As these analyses require evenly spaced samples in the series, we resampled the $\delta^{13}C$ curve of the Marne a Fucoidi with the average resolution of the original sampling (10 cm). This operation may induce some artifacts in the results, like aliasing, or the occurrence of peaks that do not correspond to a real signal. As these artifacts depend on the sampling frequency we resampled the series also with different sampling frequencies in order to check the consistency of the significant peaks.

[17] Before calculating the power spectral densities we also removed the linear trend and divided the thickness by the sedimentation rate (0.5 cm/kyr) in order to obtain periodicities in kyr.

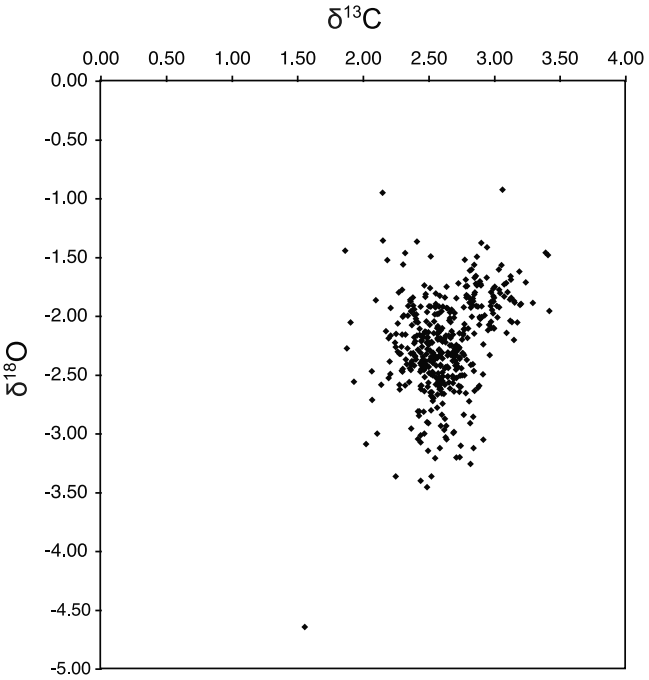

Figure 5. Crossplot of the bulk carbonate $\delta^{13}C$ versus $\delta^{18}O$ of the Albian Marne a Fucoidi.

[18] We calculated the Blackman-Tukey power spectrum using a Bartlett window, zero padding up to 2048 points, and an autocovariance calculated on 50% of the series. We also tested the reliability of the results changing these parameters and noted no significant differences in the outcomes. In every spectrum we calculated the 95% confidence level as the upper error bound of the quadratic fit. This may induce a slight underestimation of the significance of the peaks [*Weedon*, 2003], however this does not affect the main outcome in this case. In addition, we calculated the wavelet power spectrum using a Morlet wavelet and scales between 1 and 120. We also tested different number of scales in order to find the optimal solution.

5. Results

5.1. Carbon and Oxygen Isotope Data

[19] The carbonate $\delta^{13}C$ curve of the Albian Marne a Fucoidi displays an evident cyclic pattern, with values varying between 2.2‰ and 2.9‰ in the segment of Monte Petrano, and between 1.5‰ and 3.4‰ in the segment of the Piobbico core (Figure 4). We recognized the same $\delta^{13}C$ highs and lows also in the interval of *Tiraboschi et al.* [2009] that corresponds to our Monte Petrano segment, supporting the correlation between the two sections. However, the $\delta^{13}C$ pattern looks more irregular in the uppermost 8 m of the *Tiraboschi et al.* [2009] record because of the poorer preservation of this interval (see section 3.3). Counting the $\delta^{13}C$ lows in our composite section we identified 19 cycles with an average thickness of 2 m (Figure 4). The thickness of the cycles is rather constant, only cycles 3 and 11 are thicker and reach about 3m. These two thicker cycles are coupled with peculiar stratigraphic features: lithology in cycle 3 is richer in carbonate than the rest of the succession, whereas cycle 11 contains a red bed, which also displays very stable $\delta^{13}C$ values. The lowest $\delta^{13}C$ values occur at cycle 18 and between cycle 12 and 11, which are also the intervals with more black shale layers. The cyclic pattern of the $\delta^{13}C$ curve fades at the top of the Marne a Fucoidi, with the transition to the overlaying Scaglia Bianca.

[20] Oxygen isotope values vary between −3.4‰ and −1.4‰ in the segment of Monte Petrano, and between −3.1‰ and −0.9‰, in the segment of Piobbico core, with an outlier of −4.7‰, (not shown). The curve displays long- and short-term fluctuations but no defined cyclicity, for this reason we do not consider oxygen isotope data any further in this work.

5.2. Significance of the Carbon Isotope Data

[21] The carbon isotopic composition of the bulk carbonate of the Marne a Fucoidi Formation shows no covariance with $CaCO_3$ content or with $\delta^{18}O$, indicating no diagenetic alteration of the observed signal (Figures 5 and 6). Lower $\delta^{13}C$ values tend to occur in intervals with alternating black shale - limestone couplets relatively richer in black shales. However, individual black shale beds containing more organic carbon and corresponding lower $CaCO_3$ are not depleted in ^{13}C, as demonstrated in the $CaCO_3$ - $\delta^{13}C$ crossplot (Figure 6). This indicates that $\delta^{13}C$ values are not controlled by the lithology, but rather that black shale formation was favored during periods of lower $\delta^{13}C$. We thus conclude that the cyclic pattern in the $\delta^{13}C$ curve reflects changes in the isotopic composition of the dissolved inorganic carbon in the photic zone of the Tethys during the Albian. If average mixing time of Cretaceous ocean is assumed to be similar to the present, in the order of 10^3 years, then observed C-isotope changes, in the order of 10^5 years, record variations in the isotopic composition of the whole ocean inorganic carbon reservoir.

[22] The amplitude of the $\delta^{13}C$ cycles in the Piobbico core is slightly larger than in the Monte Petrano section. This

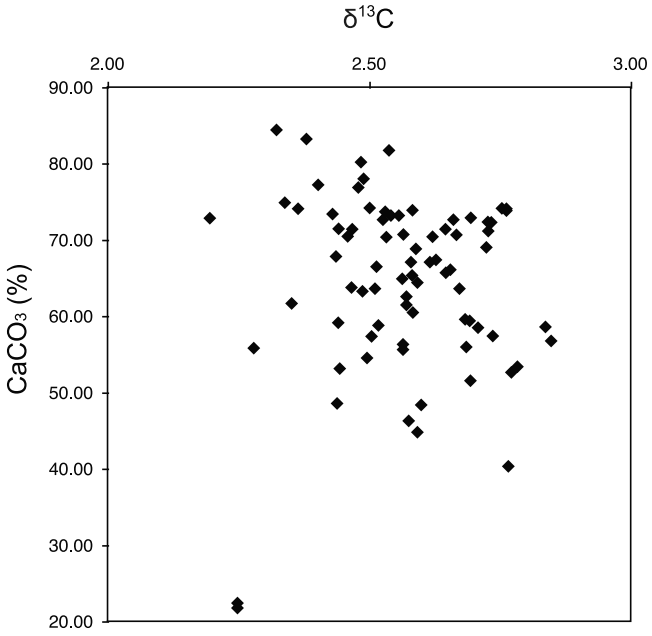

Figure 6. Crossplot of the bulk carbonate $\delta^{13}C$ versus $CaCO_3$ content measured in the intervals A, B, and C in Figure 4.

change in amplitude does not occur in the upper part of the δ^{13}C curve of *Tiraboschi et al.* [2009], which corresponds to cycles 5 to 11 of our Monte Petrano segment. We do not see a primary process that can explain such a change, so we attribute the different amplitude of the cycles to a slightly different preservation of the carbon isotopic signals between outcrop and core. This difference, though observable, does not alter the primary signal significantly.

[23] *Herbert and Fischer* [1986] estimated an average sedimentation rate for the Marne a Fucoidi of 0.5 cm/kyr. According to this estimate the average sampling resolution of our record is 20 kyr and the duration of a cycle in the δ^{13}C record is 400 kyr. Although based only on an 8 m long segment the estimate of *Herbert and Fischer* [1986] is the only one available that is independent of a cyclostratigraphic model, so it is the only tool we can use to infer the duration of the observed cycles. However, this estimate is in agreement with biostratigraphic data of *Premoli Silva and Sliter* [1995] and there are no evidences that this estimate may not be valid for the entire studied interval, in fact the quite stable thickness of the δ^{13}C cycles suggests rather the opposite. Besides, this assumption is consistent with the estimates inferred form other cyclostratigraphic models [*Fiet et al.*, 2001; *Grippo et al.*, 2004]. We discuss the possible implications of sedimentation rate variability in the following sections.

5.3. Blackman-Tukey and Wavelet Power Spectra

[24] Our δ^{13}C data can be considered as a series varying through time, so spectral analyses can be used to determine the occurrence of periodic components. We performed spectral analyses on the δ^{13}C time series both of the entire Marne a Fucoidi and of the Monte Petrano and Piobbico segments separately. The analysis of the entire Marne a Fucoidi time series has the advantage that a longer time window can be investigated, so that it is possible to detect longer periodicities. On the other hand this time series has a higher probability of being affected by artifacts, because it was constructed by merging the time series of the two separated segments, which were produced independently. Therefore we rely more on the spectra of the δ^{13}C of the two separated segments, even if based on a shorter time window.

[25] Blackman-Tukey spectra calculated on the δ^{13}C curve of the Albian Marne a Fucoidi display a prominent peak close to the 400 kyr period, which occurs consistently in the spectra both of the entire section and of the two separated segments (Figure 7). This peak is split in two subpeaks in the spectrum of the whole time series: a major peak at 382.8 kyr and a minor peak at 431.2 kyr. We interpret this as an artifact, because the minor peak is rather sensitive to changes in the number of lags used to calculate the autocovariance. However, this does not change the evidence of a strong periodic component occurring close to 400 kyr.

[26] Minor peaks occur close to the 100 kyr periodicity, barely reaching the 95% confidence level. They might represent a periodic component of the primary signal, which is, however, too weak to be confidently detected.

[27] Significant peaks also occur at low frequencies but they differ between the different spectra. These frequencies might represent artifacts or actual periodic components of the primary signal, but they are too close to the detection limit to be interpreted with confidence.

[28] Wavelet analysis allows us to determine whether the periodic signal occurring in a time series changes its periodicity throughout the series or if it is stationary. Wavelet power spectra display a strong signal around the 0.0025 frequency, corresponding to the 400 kyr period (Figure 7). In every spectrum this signal is stable and shows no shifts toward higher or lower frequencies. Therefore wavelet analysis confirms that the 400 kyr periodicity occurs in the δ^{13}C record of the Albian Marne a Fucoidi and reveals that it is consistent throughout the entire interval.

[29] The uppermost part of the *Tiraboschi et al.* [2009] δ^{13}C curve is affected by the poorer quality of the record (sections 3.3 and 5.1). Excluding this part from the calculations, spectral analyses on the *Tiraboschi et al.* [2009] record give results consistent with those in Figure 7 (not shown).

5.4. Carbon Isotope Data and Eccentricity

[30] In this study we wanted to test whether the 400 kyr cycles observed in our δ^{13}C record reflect variation in orbital eccentricity cycles like those observed in Cenozoic records [e.g., *Pälike et al.*, 2006], therefore we correlated our δ^{13}C curve with the updated version of the insolation curve of *Laskar et al.* [2004]. This version does not differ from the more recent one for the time interval considered in this work [*Laskar et al.*, 2011]. We applied a filter to both data series, in order to isolate the 400 kyr periodicity and make the long-eccentricity cycles more visible (Figure 4). The two filtered curves were then correlated according to the following assumptions:

[31] 1. We considered a constant sedimentation rate of 0.5 cm/kyr throughout the entire studied interval [*Herbert and Fischer*, 1986]. Accordingly 2 m in the Marne a Fucoidi are equal to 400 kyr in the eccentricity-time series of *Laskar et al.* [2004].

[32] 2. Since there are no numerical age tie points in the Marne a Fucoidi, we placed the base of the Albian at 112.0 $\pm$ 1.0 Myr according to *Gradstein et al.* [2004]. We use this as an arbitrary reference from which to start the correlation, but we do not claim that this is the best estimate for the base of the Albian, which is still under debate [*Gale et al.*, 2011]. A different age however would have no influence on the relationship between the δ^{13}C and eccentricity curves.

[33] 3. As the phase link between δ^{13}C and eccentricity is unknown in the Albian, we chose the correlation observed in the Cenozoic curves, where δ^{13}C minima correspond to eccentricity maxima [*Cramer et al.*, 2003; *Pälike et al.*, 2006].

[34] We tuned the two curves according to assumption 1, and tied the stratigraphically lowest δ^{13}C maximum to the eccentricity minimum closest to the 112.0 Myr ago, according to assumptions 2 and 3 (Figure 4). Reversed eccentricity and δ^{13}C curves are in phase at cycle n. 19, because of assumptions 2 and 3. They become slightly lagged toward the top of the section, with the δ^{13}C delayed in respect to the eccentricity. The lag increases gradually till cycle 14, and then decreases until cycle 11 and 12, where the curves are in phase again. Afterwards the curves show a lag, but with the δ^{13}C preceding the eccentricity. The lag increases gradually till cycle 7, and then decreases till cycle 4. Cycle 3 is larger than the others and its maximum is in phase with the corresponding eccentricity minimum, but the minimum of cycle 3

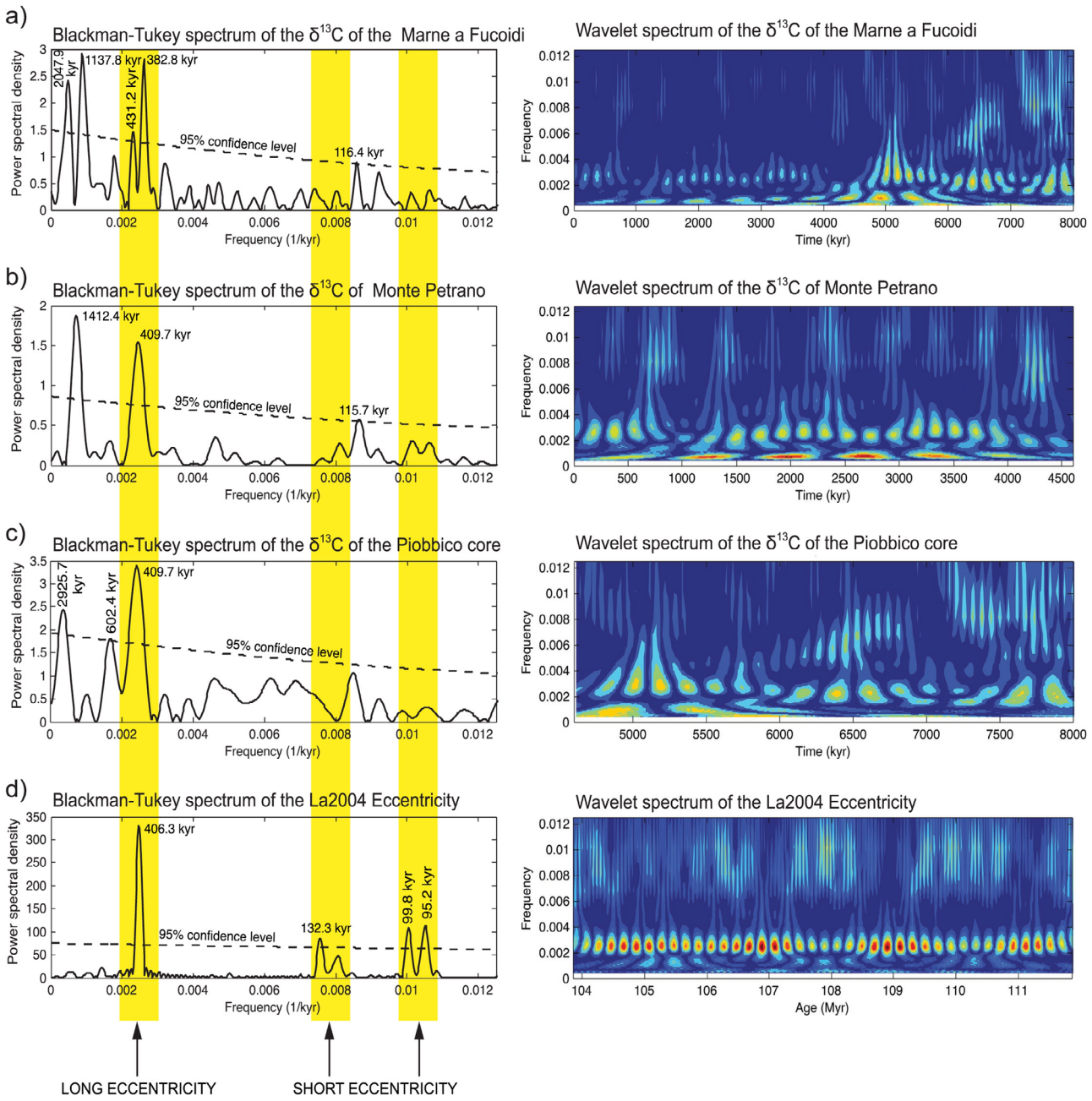

Figure 7. (left) Blackman-Tukey and (right) wavelet power spectra of (a) the δ^{13}C curve of the entire Albian Marne a Fucoidi, (b) the δ^{13}C curve of the Monte Petrano segment, (c) the δ^{13}C curve of the Piobbico core segment, and (d) the La2004 eccentricity curve.

is advanced and that of cycle 4 is delayed with respect to the corresponding eccentricity maxima. At cycle 1 the δ^{13}C is still delayed with respect to eccentricity, but less than at cycle 2. The phase-lag between δ^{13}C and eccentricity is variable but is always less than half a cycle (200 kyr).

[35] The observed phase-lags between the δ^{13}C and eccentricity curves are probably due to the constant sedimentation rate approximation (assumption 1). It is indeed unlikely that the sedimentation rate of the Marne a Fucoidi remained constant over nearly 8 Myr, so the temporal signal in the δ^{13}C is probably slightly distorted by variations in the sedimentation rate. One evidence for distortion is that within the cycle 11 the 400 kyr-filtered δ^{13}C curve displays another cycle that does not appear in the unfiltered curve. This suggests that the red bed and the very stable δ^{13}C values in cycle 11 reflect condensation, or at least a reduced sedimentation rate. On the other hand, cycle 3, which is nearly 3 m thick and corresponds to a more carbonate-rich facies, is probably related to increased sedimentation rate. In the Oligocene, *Pälike et al.* [2006] observed a nearly 20 kyr lag between the δ^{13}C and δ^{18}O curves for long-eccentricity cycles. It remains unknown if such a lag existed in the Albian, but if it is the case then it could contribute to the partial decoupling we observed. However, the phase-lags are

always smaller than half a cycle, so they create no ambiguity in the correlation between the $\delta^{13}C$ minima and the corresponding eccentricity maxima. This indicates that the approximation of a constant sedimentation rate does not create a significant bias and also highlights the strong stability of the 400 kyr signal in the carbon isotope data. Spectral analyses performed on the *Laskar et al.* [2004] eccentricity-time series show the 400 kyr as the dominant periodicity of eccentricity variations and confirm their tight link with $\delta^{13}C$ (Figure 7).

6. Discussion

6.1. Milankovitch Cycles in the Marne a Fucoidi

[36] Since the work of *Herbert and Fischer* [1986] the Marne a Fucoidi Formation has been considered as one of the best geological records displaying Milankovitch cycles. Alongside lithological couplets and bundles, these cycles have been recognized in variations in $CaCO_3$ and aluminum contents [*Herbert*, 1997], as well as in calcareous nannofossil abundances [*Erba*, 1992; *Tiraboschi et al.*, 2009], and in some redox-sensitive elements [*Tateo et al.*, 2000; *Galeotti et al.*, 2003]. However, previous studies identified mainly precession and short-eccentricity rather than long-eccentricity.

[37] The most detailed study of Milankovitch cycles in the Marne a Fucoidi published so far is that by *Grippo et al.* [2004], who studied the lithological variations in the Piobbico core using a photo-scanning technique. In Figure 8 we compare our data set with that of *Grippo et al.* [2004]. We used the base of the Urbino level, the base of the second red bed, and the boundary with the Scaglia Bianca as reference horizons for correlation. Because the lower segment of our section is also from the Piobbico core it corresponds exactly with the stratigraphic log of *Grippo et al.* [2004], whereas the segment of Monte Petrano is nearly 2 m thicker than its counterpart due to a slightly higher sedimentation rate in Monte Petrano and/or some missing part in the upper meters of the Piobbico core (see section 3.3). This indicates a maximum difference in sedimentation rate of 0.05 cm/kyr between Piobbico and Monte Petrano, which would change the duration of the cycles by about 25 kyr. This uncertainty is slightly higher than our sampling resolution and does not bias significantly the correlation and the results.

[38] Despite the good lithological correlation, the number of 400 kyr cycles is slightly different between our record and that of *Grippo et al.* [2004]. Considering that our cycle 11 represents two 400 kyr cycles (see section 5.4), we found twelve cycles in the upper segment instead of the thirteen of *Grippo et al.* [2004]. In the lower segment, on the contrary, we found only eight cycles instead of the ten of *Grippo et al.* [2004]. This mismatch is due to the different methodology used to identify the 400 kyr cycles: we identified them directly from the $\delta^{13}C$ curve, whereas *Grippo et al.* [2004] extrapolated their boundaries by grouping 100 kyr cycles, which are better recognizable in their data set. Moreover, *Grippo et al.* [2004] assumed condensation in their cycles 7, 27, and 30, and a gap due to a fault between their cycles 21 and 22, so they added an unspecified number of 100 kyr cycles in these intervals to take this into account. Consequently, they obtained thinner and a higher number of 400 kyr cycles. On the other hand, we observed condensation only in our cycle 11, whereas the thickness of the cycles is stable in the rest of our data set and also cycle 13, in the part of the core affected by the fault, does not show an anomalous thickness. Thus we did not consider necessary to add hypothetical cycles compensating for gaps or condensation.

[39] Although we cannot completely exclude the possibility that some 400 kyr cycles are missing also in our section, we have two reasons to consider the 400 kyr cycles identified in the $\delta^{13}C$ as more reliable than the lithological cycles:

[40] 1. Super-bundles corresponding to long eccentricity cycles are not directly identifiable in the lithological record and need to be derived by shorter-term rhythms (couplets and bundles). This induces uncertainty in the recognition of the 400 kyr cycles, as acknowledged also by *Fiet et al.* [2001] who counted fourteen bundles, or three and half super-bundles, less in Monte Petrano than in the Piobbico core. The $\delta^{13}C$-curve, on the other hand, displays a much more regular and stable signal in which maxima and minima of the cycles are rather easy to recognize. This is due to the lower sensitivity of carbon isotope values in pelagic settings to rapid and local effects, which makes this the best tool to identify 400 kyr cycles in fossil records [*Cramer et al.*, 2003].

[41] 2. The correlation between our $\delta^{13}C$ curve and the *Laskar et al.* [2004]'s eccentricity curve is straightforward, as they display the same number of cycles and are also rather in phase. Although uncertainties still exist there is no further evidence to assume that some cycle is missing. These observations might also be useful for further studies on the orbital tuning of the Albian stage, like that of *Gale et al.* [2011].

6.2. Long Eccentricity Cycles in Carbon Isotope Records

[42] Long eccentricity cycles have been recognized in several carbon isotope records throughout the Cenozoic, both under greenhouse and under icehouse conditions [e.g., *Zachos et al.*, 2001; *Cramer et al.*, 2003; *Holbourn et al.*, 2005; *Pälike et al.*, 2006]. These cycles are from 0.5‰ to 1.0‰ in amplitude and their minimum values are correlated with maxima in eccentricity. They show that the oceanic carbon reservoir is sensitive to orbital forcing and it responds with the long eccentricity period because of the 10^5 years long residence time of inorganic carbon in the ocean [*Cramer et al.*, 2003]. Interestingly the tight phase relationship between high $\delta^{13}C$ and low eccentricity becomes obscured around 1.6 Ma ago, at the onset of the Quaternary glacial cycles [*Wang et al.*, 2010].

[43] Many Cretaceous deep-water records display rhythms related to Milankovitch cycles in lithology and other climatic proxies [e.g., *Herbert*, 1997; *Tateo et al.*, 2000; *Köβler et al.*, 2001]. On the other hand only few authors so far noticed their presence in carbon isotope records [*Sprovieri et al.*, 2006; *Voigt et al.*, 2007]. These authors hypothesized a link between long eccentricity and carbon cycle, but did not test whether their $\delta^{13}C$ curves correlated with a paleoeccentricity model, nor did they discuss possible paleoclimatic implications.

[44] In this study we have shown that a link between eccentricity and the carbon cycle, as observed in the Cenozoic, also existed in the mid-Cretaceous. This indicates that comparable mechanisms were acting in periods considered very different in terms of climatic and oceanographic

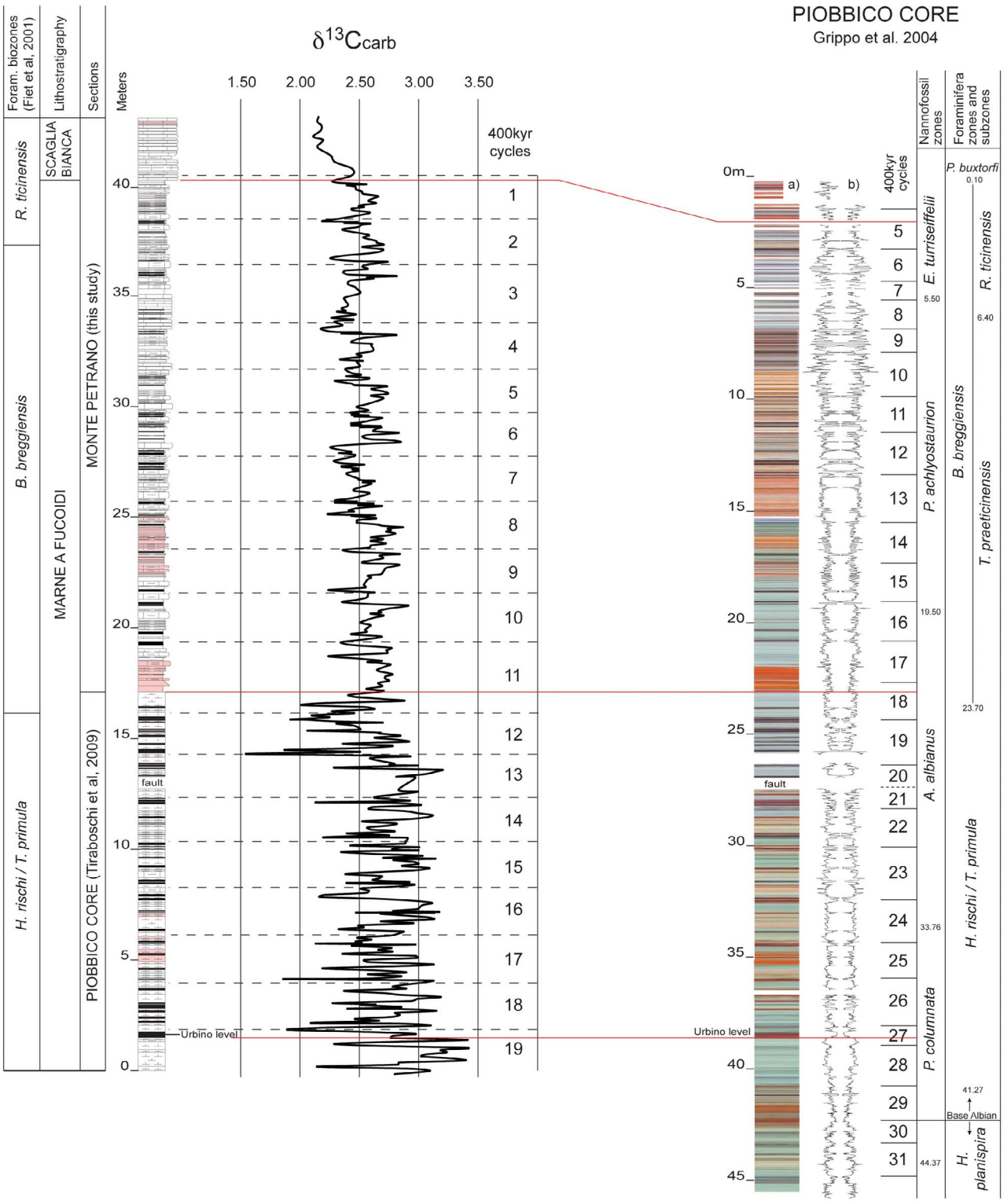

Figure 8. Comparison between 400 kyr cycles in the Marne a Fucoidi identified in the $\delta^{13}C$ record of (left) this study and (right) in the lithological record of *Grippo et al.* [2004]. (a) Photolog with stratigraphic depth and (b) butterfly plot widens to white, and constricts to dark colors.

conditions. So, which mechanisms coupling carbon cycle and orbital parameters could have been active both in the Cenozoic and in the mid-Cretaceous?

[45] A definite answer to this question is hampered both by our limited knowledge of the Cretaceous ocean and climate dynamics, and by the uncertainties that still exist about the mechanisms that make the carbon cycle respond to

eccentricity changes. Although the occurrence of short glacial episodes during the mid-Cretaceous is currently under debate, paleotemperature proxies suggest very warm temperatures and absence of permanent ice sheets during most of the investigated interval [*Pucéat et al.*, 2003; *Erbacher et al.*, 2011]. Under these conditions, the absence of permanent low-pressure fronts at the poles implies that climate becomes more sensitive to monsoonal dynamics, such as sea-land pressure gradients driving air mass circulation and moisture transport [e.g., *Barron et al.* 1985; *Hay*, 2008]. Therefore the monsoonal system was probably much more important under the mid-Cretaceous climatic conditions than it is today. As the monsoonal system is strongly controlled by orbital variations, which modulate seasonal contrasts, it is probable that widespread orbital cycles recorded in mid-Cretaceous archives testify to a monsoonal activity much more intense and widespread than today. This hypothesis was already considered as explanation for the mid-Cretaceous black shales occurring in the Umbria-Marche and Vocontian basins [*Pratt and King*, 1986; *Herrle et al.*, 2003].

[46] A link between global monsoonal system and carbon cycle was proposed to explain long eccentricity cycles in Cenozoic carbon isotope records [*Holbourn et al.*, 2007; *Wang*, 2009; *Zachos et al.*, 2010; *Ma et al.* 2011]. We hypothesize that similar mechanisms existed also in the mid-Cretaceous, whereby intervals of δ^{13}C minima were related to eccentricity maxima and reflect periods of stronger seasonal contrast, with more intense monsoonal activity. More intense deep-water circulation triggered by more seasonal climate could have reduced organic carbon burial rates and decreased the carbon isotope composition of seawater on a global scale. Besides, an increase in the flux of isotopically light carbon from the land to the ocean could have contributed to lower carbon isotope values. This is also supported by the fact that δ^{13}C minima in the Marne a Fucoidi tend to coincide with intervals containing more black shales. These black shales contain organic matter of mainly terrestrial origin that was probably delivered into the basin by intense winds [*Pratt and King*, 1986]. Another possibility to explain the monsoon-carbon cycle link is that during eccentricity minima more prolonged wet seasons favored carbon accumulation in wetlands, which sequestered ^{13}C-depleted carbon and led to an increase in the δ^{13}C of dissolved inorganic carbon in the ocean [*Zachos et al.*, 2010].

[47] The next question is why the 400 kyr cycles cease to be recorded at the onset of the Scaglia Bianca Formation. A change in facies accompanied by a change in δ^{13}C suggests that the new sedimentation mode is the local expression of an event involving the whole oceanic carbon reservoir. If the hypothesis that the 400 kyr cycles in δ^{13}C represent the response of the oceanic carbon reservoir to monsoonal activity is true, then the disappearance of these cycles from the fossil record means either a weakening of the monsoonal activity or a change in the ocean system that reduced its sensitivity to orbital forcing. A weaker monsoonal activity could have been due to the formation of seaways, which disrupted the sea-land pressure gradients in the northern hemisphere from the mid- to the Late Cretaceous [*Park and Oglesby*, 1994]. An alternative explanation can be a major change in the Tethyan oceanography, possibly related to a reorganization of the global oceanic system. As described also by *Wang et al.* [2004, 2010] the response of the oceanic carbon reservoir to orbital forcing it is strongly dependent on the structure of the ocean. This means that the arrangement of upwelling and deep water formation sites, the water mixing rates, the stability of the circulation patterns and of the stratification of the water column determine the sensitivity of the oceanic carbon system to external forcing. A rather homogeneous sedimentation coupled with δ^{13}C values that are stable and close to those of the cycles minima, suggests a more stable circulation of low latitude oceans, with a deep thermocline and enhanced ventilation of the bottom waters. This more stable circulation mode would have made the oceanic system less sensitive to orbital changes. For the Albian this last explanation is more likely because this period was characterized by opening and widening of oceanic gateways and by a long-term sea level rise. These factors might have enhanced the water exchange between the different ocean basins and so triggered a major change in oceanic circulation [e.g., *Poulsen et al.*, 2001].

7. Conclusions

[48] In this study we present new lithological and isotope data of the Albian interval of the Marne a Fucoidi Formation, which is one of the most detailed sedimentary records of the mid-Cretaceous. Carbon isotope values display prominent 400 kyr cycles, which correlate with the long eccentricity cycles, resembling those observed in several Cenozoic records. This suggests that the Cretaceous carbon cycle responded to orbital eccentricity changes in the same way as in the Cenozoic, despite different climatic and oceanographic boundary conditions. We postulate that the observed cycles reflect variations in the oceanic carbon budget driven by orbitally modulated monsoonal activity. This suggests that during the mid-Cretaceous the climate was strongly controlled by orbital variations but also that the oceanic system was highly sensitive to these changes. The disappearance of the 400 kyr cycles from the δ^{13}C record in the Late Albian suggests a major rearrangement of the structure of the ocean.

[49] **Acknowledgments.** We thank E. Erba and D. Tiraboschi from the University of Milan for having provided the data of the Piobbico core. We are grateful to M. Coray and S. Bishop for the technical assistance in the laboratory and to N. Deichmann for the help in spectral analyses. Financial support from the Swiss National Science Foundation (grant 02-77104-07) is gratefully acknowledged. We thank also Andy Gale and an anonymous reviewer who helped improve the manuscript.

References

Arthur, M. A., and I. Premoli Silva (1982), Development of widespread organic carbon-Rich strata in the Mediterranean Tethys, in *Nature and Origin of Cretaceous Carbon-Rich Facies*, edited by S. O. Schlanger and M. B. Cita, pp. 6–54, Academic, London.

Barron, E. J., M. A. Arthur, and E. G. Kauffman (1985), Cretaceous rhythmic bedding sequences: A plausible link between orbital variations and climate, *Earth Planet. Sci. Lett.*, *72*, 327–340, doi:10.1016/0012-821X(85)90056-1.

Bice, K. L., and R. D. Norris (2002), Possible atmospheric CO_2 extremes of the Middle Cretaceous (late Albian-Turonian), *Paleoceanography*, *17*(4), 1070, doi:10.1029/2002PA000778.

Bice, K. L., D. Birgel, P. A. Meyers, K. A. Dahl, K.-U. Hinrichs, and R. D. Norris (2006), A multiple proxy and model study of Cretaceous upper ocean temperatures and atmospheric CO_2 concentrations, *Paleoceanography*, *21*, PA2002, doi:10.1029/2005PA001203.

Coccioni, R. (1996), The Cretaceous of the Umbria-Marche Apennines (central Italy), in *Cretaceous Stratigraphy, Paleobiology and Paleobiogeography: Abstracts: Tübingen, Germany, 7–10 March 1996*, edited by J. Wiedmann, pp. 129–136, Geol.-Paläontologisches Instit. und Mus., Christian-Albrechts-Universit., Kiel, Germany.

Coccioni, R., R. Franchi, O. Nesci, N. Perilli, F. C. Wezel, and F. Battistini (1989), Stratigrafia, micropaleontologia e mineralogia delle Marne a Fucoidi (Aptiano inferiore-Albiano superiore) delle sezioni di Poggio le Guaine e del Fiume Bosso (Appennino umbro-marchigiano), in *Proceedings of the Third Pergola International Symposium: Fossili, Evoluzione, Ambiente*, edited by G. Pallini et al., pp. 163–201, Comitato Centenario Raffaele Puccini, Pergola, Italy.

Cool, T. E. (1982), Sedimentological evidence concerning the paleoceanography of the Cretaceous western North Atlantic Ocean, *Palaeogeogr. Palaeoclimatol. Palaeoecol.*, *39*, 1–35, doi:10.1016/0031-0182(82)90070-0.

Cramer, B. S., J. D. Wright, D. V. Kent, and M.-P. Aubry (2003), Orbital climate forcing of $\delta^{13}C$ excursions in the late Paleocene–early Eocene (chrons C24n–C25n), *Paleoceanography*, *18*(4), 1097, doi:10.1029/2003PA000909.

Dean, W. E., J. V. Gardner, L. F. Jansa, P. Cepek, and E. Seibold (1977), Cyclic sedimentation along the continental margin of northwest Africa, *Initial Rep. Deep Sea Drill. Proj.*, *51*, 965–989.

Erba, E. (1992), Calcareous nannofossil distribution in the pelagic rhythmic sediments (Aptian-Albian Piobbico Core, Central Italy), *Rivista Ital. Paleontol. Stratigr.*, *97*(3–4), 455–484.

Erbacher, J., O. Friedrich, P. A. Wilson, J. Lehmann, and W. Weiss (2011), Short-term warming events during the boreal Albian (mid-Cretaceous), *Geology*, *39*(3), 223–226, doi:10.1130/G31606.1.

Fiet, N. (1998), Les black shales, un outil chronostratigraphique haute résolution. Exemple de l'Albien du bassin de Marches-Ombrie (Italie centrale), *Bull. Soc. Geol. Fr.*, *169*(2), 221–231.

Fiet, N., B. Beaudoin, and O. Parize (2001), Lithostratigraphic analysis of Milankovich cyclicity in pelagic Albian deposits of central Italy: Implications for the duration of the stage and substages, *Cretaceous Res.*, *22*, 265–275, doi:10.1006/cres.2001.0258.

Fischer, A. G., T. D. Herbert, G. Napoleone, I. Premoli Silva, and M. Ripepe (1991), Albian pelagic rhythms (Piobbico Core), *J. Sediment. Petrol.*, *61*(7), 1164–1172.

Gale, A. (1989), A Milankovitch scale for Cenomanian time, *Terra Nova*, *1*, 420–425, doi:10.1111/j.1365-3121.1989.tb00403.x.

Gale, A., P. Bown, M. Caron, J. Crampton, S. J. Crowhurst, W. J. Kennedy, M. R. Petrizzo, and D. S. Wray (2011), The uppermost middle and upper Albian succession at the Col de Palluel, Hautes-Alpes, France: An integrated study (ammonites, inoceramid bivalves, planktonic foraminifera, nannofossils, geochemistry, stable oxygen and carbon isotopes, cyclostratigraphy), *Cretaceous Res.*, *32*, 59–130, doi:10.1016/j.cretres.2010.10.004.

Galeotti, S., M. Sprovieri, R. Coccioni, A. Bellanca, and R. Neri (2003), Orbitally modulated black shale deposition in the upper Albian Amadeus Segment (central Italy): A multi-proxy reconstruction, *Palaeogeogr. Palaeoclimatol. Palaeoecol.*, *190*, 441–458, doi:10.1016/S0031-0182(02)00618-1.

Gradstein, F. M., J. G. Ogg, and A. G. Smith (2004), *A Geologic Time Scale 2004*, edited by F. M. Gradstein, J. G. Ogg, and A. G. Smith, 500 pp., Cambridge Univ. Press, Cambridge, U. K.

Grippo, A., A. G. Fischer, L. A. Hinnov, T. D. Herbert, and I. Premoli Silva (2004), Cyclostratigraphy and Chronology of the Albian Stage (Piobbico core, Italy), in *Cyclostratigraphy: Approaches and Case Histories*, edited by B. D'Argenio et al., *SEPM Spec. Publ.*, *81*, 57–81.

Hardenbol, J., J. Thierry, M. B. Farley, T. Jacquin, P. C. De Graciansky, and P. R. Vail (1998), Mesozoic and Cenozoic sequence chronostratigraphic chart, in *Mesozoic and Cenozoic Sequence Stratigraphy of European Basins*, *SEPM Spec. Publ.*, *60*, 363–364.

Hay, W. (2008), Evolving ideas about the Cretaceous climate and ocean circulation, *Cretaceous Res.*, *29*, 725–753, doi:10.1016/j.cretres.2008.05.025.

Herbert, T. D. (1997), A long marine history of carbon cycle modulation by orbital-climatic changes, *Proc. Natl. Acad. Sci. U. S. A.*, *94*, 8362–8369, doi:10.1073/pnas.94.16.8362.

Herbert, T. D., and A. G. Fischer (1986), Milankovitch climatic origin of the mid-Cretaceous black shale rhythms in central Italy, *Nature*, *321*, 739–743, doi:10.1038/321739a0.

Herrle, J. O., J. Pross, O. Friedrich, P. Kößler, and C. Hemleben (2003), Forcing mechanisms for mid-Cretaceous black shale formation: Evidence from the upper Aptian and lower Albian of the Vocontian Basin (SE France), *Palaeogeogr. Palaeoclimatol. Palaeoecol.*, *190*, 399–426, doi:10.1016/S0031-0182(02)00616-8.

Holbourn, A., W. Kuhnt, M. Schulz, and H. Erlenkeuser (2005), Impacts of orbital forcing and atmospheric carbon dioxide on Miocene ice-sheet expansion, *Nature*, *438*, 483–487, doi:10.1038/nature04123.

Holbourn, A., W. Kuhnt, M. Schulz, J. Flores, and N. Andersen (2007), Orbitally paced climate evolution during the middle Miocene "Monterey" carbon-isotope excursion, *Earth Planet. Sci. Lett.*, *261*, 534–550, doi:10.1016/j.epsl.2007.07.026.

Hu, X., L. Jansa, and M. Sarti (2006), Mid-Cretaceous oceanic red beds in the Umbria-Marche Basin, central Italy: Constrains on paleoceanography and paleoclimate, *Palaeogeogr. Palaeoclimatol. Palaeoecol.*, *233*, 163–186, doi:10.1016/j.palaeo.2005.10.003.

Huber, B. T., R. D. Norris, and K. G. MacLeod (2002), Deep-sea paleotemperature record of extreme warmth during the Cretaceous, *Geology*, *30*(2), 123–126, doi:10.1130/0091-7613(2002)030<0123:DSPROE>2.0.CO;2.

Jahren, A. H., N. C. Arens, G. Sarmiento, J. Guerrero, and R. Amundson (2001), Terrestrial record of methane hydrate dissociation in the Early Cretaceous, *Geology*, *29*, 159–162, doi:10.1130/0091-7613(2001)029<0159:TROMHD>2.0.CO;2.

Kößler, P., J. O. Herrle, E. Appel, J. Erbacher, and C. Hemleben (2001), Magnetic records of climatic cycles from mid-Cretaceous hemipelagic sediments of the Vocontian Basin, SE France, *Cretaceous Res.*, *22*, 321–331, doi:10.1006/cres.2001.0256.

Larson, R. L., and E. Erba (1999), Onset of the mid-Cretaceous greenhouse in the Barremian-Aptian: Igneous events and the biological, sedimentary, and geochemical responses, *Paleoceanography*, *14*(6), 663–678, doi:10.1029/1999PA900040.

Laskar, J., P. Robutel, F. Joutel, M. Gastineau, A. C. M. Correia, and B. Levrard (2004), A long-term numerical solution for the insolation quantities of the Earth, *Astron. Astrophys.*, *428*, 261–285, doi:10.1051/0004-6361:20041335.

Laskar, J., A. Fenga, M. Gastineau, and H. Manche (2011), La2010: a new orbital solution for the long-term motion of the Earth, *Astron. Astrophys.*, *532*, A89, doi:10.1051/0004-6361/201116836.

Lavecchia, G., and G. Pialli (1989), The Umbria-Marche arcuate fold belt, in *Stratigrafia del Mesozoico e Cenozoico nell'area Umbro-Marchigiana, Itinerari Geologici sull'Appennino Umbro-Marchigiano (Italia)*, *Mem. Desc. Della Soc. Geol. d'Ital.*, vol. 39, edited by S. Cresta, S. Monechi, and G. Parisi, pp. 10–14, Ist. Poligrafico e Zecca dello Stato, Rome.

Ma, W., J. Tian, Q. Li, and P. Wang (2011), Simulation of long eccentricity (400 kyr) cycle in ocean carbon reservoir during Miocene Climate Optimum: Weathering and nutrient response to orbital change, *Geophys. Res. Lett.*, *38*, L10701, doi:10.1029/2011GL047680.

Méhay, S., C. Keller, S. Bernasconi, H. Weissert, E. Erba, C. Bottini, and P. A. Hochuli (2009), A volcanic CO_2 pulse triggered the Cretaceous Oceanic Anoxic Event 1a and a biocalcification crisis, *Geology*, *37*(9), 819–822, doi:10.1130/G30100A.1.

Pälike, H., R. D. Norris, J. O. Herrle, P. A. Wilson, H. K. Coxall, C. H. Lear, N. J. Shackleton, A. K. Tripati, and B. S. Wade (2006), The heartbeat of the Oligocene climate system, *Science*, *314*, 1894–1898, doi:10.1126/science.1133822.

Park, J., and R. J. Oglesby (1994), The effect of orbital cycles on Late and Middle Cretaceous climate: A comparative general circulation model study, *Spec. Publ. Int. Assoc. Sedimentol.*, *19*, 509–529.

Poulsen, C., E. Barron, M. A. Arthur, and W. H. Peterson (2001), Response of the mid-Cretaceous global oceanic circulation to tectonic and CO_2 forcings, *Paleoceanography*, *16*(6), 576–592, doi:10.1029/2000PA000579.

Pratt, L. M., and J. D. King (1986), Variable marine productivity and high eolian input recorded by rhythmic black shales in Mid-Cretaceous pelagic deposits from central Italy, *Paleoceanography*, *1*(4), 507–522, doi:10.1029/PA001i004p00507.

Premoli Silva, I., and W. V. Sliter (1995), Cretaceous planktonic foraminiferal biostratigraphy and evolutionary trends from the Bottaccione section, Gubbio (Italy), *Paleontol. Ital.*, *82*, 1–89.

Prokoph, A., and J. Thurow (2001), Orbital forcing in a "Boreal" Cretaceous epeiric sea: High-resolution analysis of core and logging data (upper Albian of the Kirchrode I drill core — Lower Saxony basin, NW Germany), *Palaeogeogr. Palaeoclimatol. Palaeoecol.*, *174*, 67–96, doi:10.1016/S0031-0182(01)00287-5.

Pucéat, E., C. Lecuyer, S. M. F. Sheppard, G. Dromart, S. Reboulet, and P. Grandjean (2003), Thermal evolution of Cretaceous Tethyan marine waters inferred from oxygen isotope composition of fish tooth enamels, *Paleoceanography*, *18*(2), 1029, doi:10.1029/2002PA000823.

Sprovieri, M., R. Coccioni, F. Lirer, N. Pelosi, and F. Lozar (2006), Orbital tuning of a lower Cretaceous composite record (Maiolica Formation, central Italy), *Paleoceanography*, *21*, PA4212, doi:10.1029/2005PA001224.

Tateo, F., N. Morandi, A. Nicolai, M. Ripepe, R. Coccioni, S. Galeotti, and F. Baudin (2000), Orbital control on pelagic clay sedimentology: The case of the late Albian "Amadeus Segment" (Central Italy), *Bull. Soc. Geol. Fr.*, *171*, 217–228, doi:10.2113/171.2.217.

Tiraboschi, D., E. Erba, and H. Jenkyns (2009), Origin of rhythmic Albian black shales (Piobbico core, central Italy): Calcareous nannofossil

quantitative and statistical analyses and paleoceanographic reconstructions, *Paleoceanography*, *24*, PA2222, doi:10.1029/2008PA001670.

Tornaghi, M. E., I. Premoli Silva, and M. Ripepe (1989), Lithostratigraphy and planktonic foraminiferal biostratigraphy of the Aptian-Albian "Scisti a Fucoidi" in the Piobbico core, Marche, Italy: Background for cyclostratigraphy, *Rivista Ital. Paleontol. Stratigr.*, *95*(3), 223–264.

Trauth, M. H. (2010), *MATLAB Recipes for Earth Sciences*, 3rd ed., Springer, Heidelberg, doi:10.1007/978-3-642-12762-5.

Voigt, S., A. Aurag, F. Leis, and U. Kaplan (2007), Late Cenomanian to middle Turonian high-resolution carbon isotope stratigraphy: New data from the Münsterland Cretaceous Basin, Germany, *Earth Planet. Sci. Lett.*, *253*, 196–210, doi:10.1016/j.epsl.2006.10.026.

Wang, P. (2009), Global monsoon in a geological perspective, *Chin. Sci. Bull.*, *54*(7), 1113–1136, doi:10.1007/s11434-009-0169-4.

Wang, P., J. Tian, X. Cheng, C. Liu, and J. Xu (2004), Major Pleistocene stages in a carbon perspective: The South China Sea record and its global comparison, *Paleoceanography*, *19*, PA4005, doi:10.1029/2003PA000991.

Wang, P., J. Tian, and L. J. Lourens (2010), Obscuring of long eccentricity cyclicity in Pleistocene oceanic carbon isotope records, *Earth Planet. Sci. Lett.*, *290*, 319–330, doi:10.1016/j.epsl.2009.12.028.

Weedon, G. (2003), *Time-Series Analysis and Cyclostratigraphy*, 1st ed., Cambridge Univ. Press, Cambridge, U. K., doi:10.1017/CBO9780511535482.

Weissert, H., and E. Erba (2004), Volcanism, CO_2 and palaeoclimate: A Late Jurassic–Early Cretaceous carbon and oxygen isotope record, *J. Geol. Soc.*, *161*, 695–702, doi:10.1144/0016-764903-087.

Zachos, J. C., N. J. Shackleton, J. S. Revenaugh, H. Pälike, and B. P. Flower (2001), Climate response to orbital forcing across the Oligocene-Miocene boundary, *Science*, *292*, 274–278, doi:10.1126/science.1058288.

Zachos, J. C., H. McCarren, B. Murphy, U. Röhl, and T. Westerhold (2010), Tempo and scale of Late Paleocene and Early Eocene carbon isotope cycles: Implications for the origin of hyperthermals, *Earth Planet. Sci. Lett.*, *299*, 242–249, doi:10.1016/j.epsl.2010.09.004.

S. M. Bernasconi, M. Giorgioni, C. E. Keller, and H. Weissert, Department of Earth Sciences, Geological Institute, ETH Zurich, Sonneggstr. 5, CH-8092 Zürich, Switzerland. (stefano.bernasconi@erdw.ethz.ch; martino.giorgioni@erdw.ethz.ch; christina.keller@erdw.ethz.ch; helmut.weissert@erdw.ethz.ch)

R. Coccioni, Dipartimento di Scienze della Terra, della Vita e dell'Ambiente, Università di Urbino, I-61209 Urbino, Italy. (rodolfo.coccioni@uniurb.it)

P. A. Hochuli, Palaeontological Institute, University of Zurich, Karl Schmid-Strasse 4, CH-8006 Zürich, Switzerland. (peter.hochuli@erdw.ethz.ch)